

In the nuclear industry, zirconium (Zr) alloys are the material of choice for fuel cladding and reactor channels. To enhance performance and lifespan of the channels and the reactor, it is vital to know how alloy composition and thermal processing influence the formation of secondary phase particles (SPPs). GE Hitachi and Global Nuclear Fuel GNF are currently investigating the phase transformations in a specific Zr alloy, NSF (1wt%Nb-1wt%Sn-0.4wt%Fe). Pertaining to this project, NSF samples were heat treated at various temperatures and times, and the subsequent effects of these heat treatments on the microstructure and phase transitions were observed using multiple characterization methods, including differential scanning calorimetry (DSC), x-ray diffraction (XRD), scanning electron microscopy (SEM), and transmission electron microscopy (TEM).

This work is sponsored by GE Hitachi and Global Nuclear Fuel



**Project Background:** The use of Zr alloys in boiling water nuclear reactors has been well documented due to their low absorption cross-section of thermal neutrons and corrosion resistance [1,2]. Cladding channels are structural components that support the uranium containing fuel rods within the reactor. Currently, these channels are fabricated from both Zircaloy-2&4 Zr alloys. Unfortunately, these alloys cause interference issues due to geometrical distortion caused by fluence gradient-induced bow. This distortion leads to control blade interference and potential safety issues as illustrated in Figure 1. Due to this, a new Zr alloy, termed NSF(Zr-1Nb-1Sn-0.35Fe), is being considered by GNF as a substitute for the current channel material because it exhibits a high resistance to fluence gradient induced bowing [3]. Current research has demonstrated that the corrosion behavior of Nb containing alloys is sensitive to the microstructure [4] and, therefore, it is of great interest to understand the response of SPPs during thermal processing of this novel Zr alloy. Characterization of the microstructures and the phase transformation was performed to understand SPP behavior.

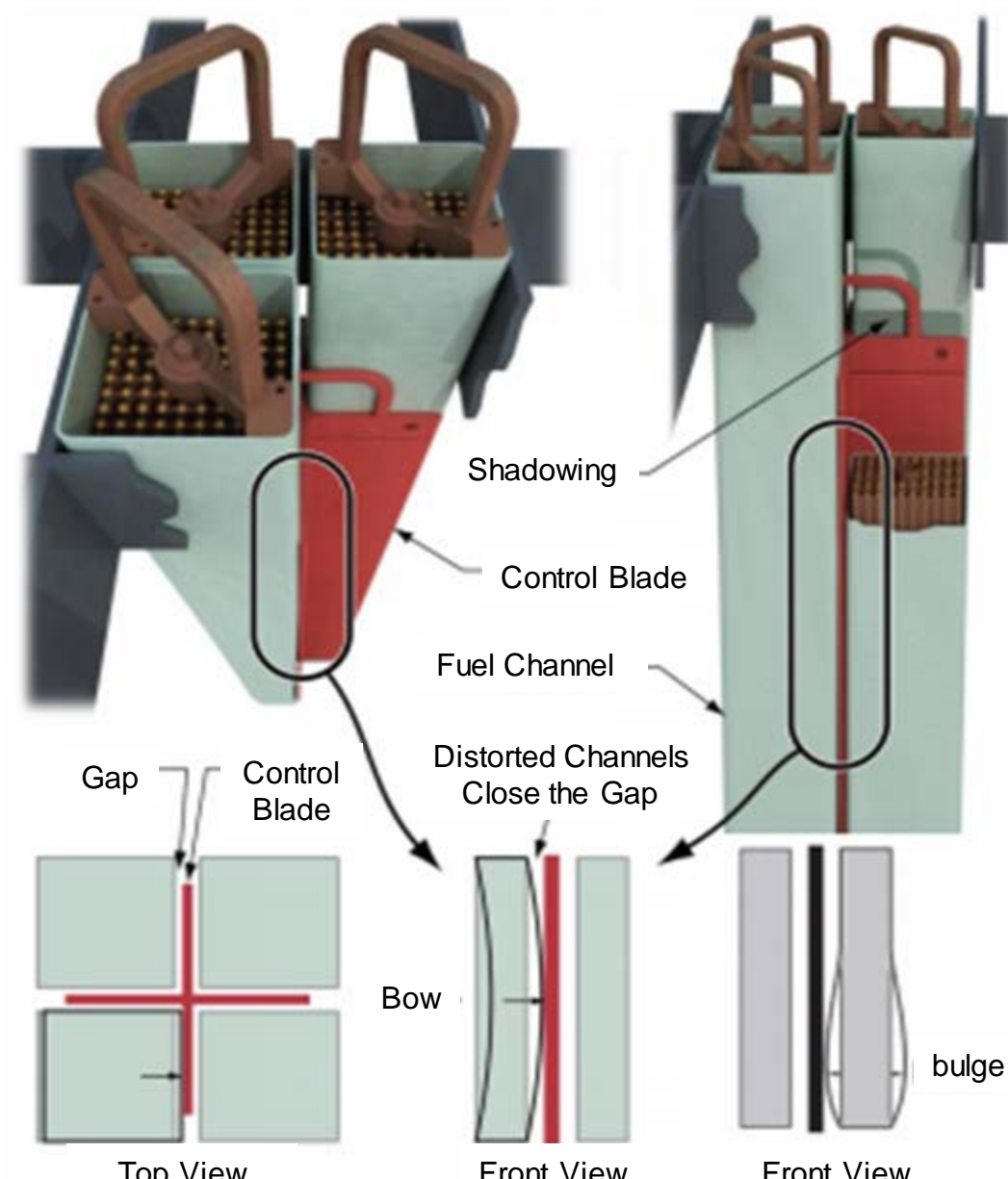


Figure 1. Illustration of the fuel cladding channels and geometric distortion[3].

**X-Ray Diffraction:** The XRD analysis was carried out on samples of heat treated and  $\beta$ -quenched NSF alloys (a Bruker D8 Focus X-Ray Diffractometer, Madison, WI) and were compared (Figure 3). According to Kim et al [5] if the  $\beta_{Nb}$  phase precipitated then the corresponding (110) peak at  $38.2^\circ$  would be found. A more thorough scan of the  $2\theta$  range of interest showed that this phase is not present.

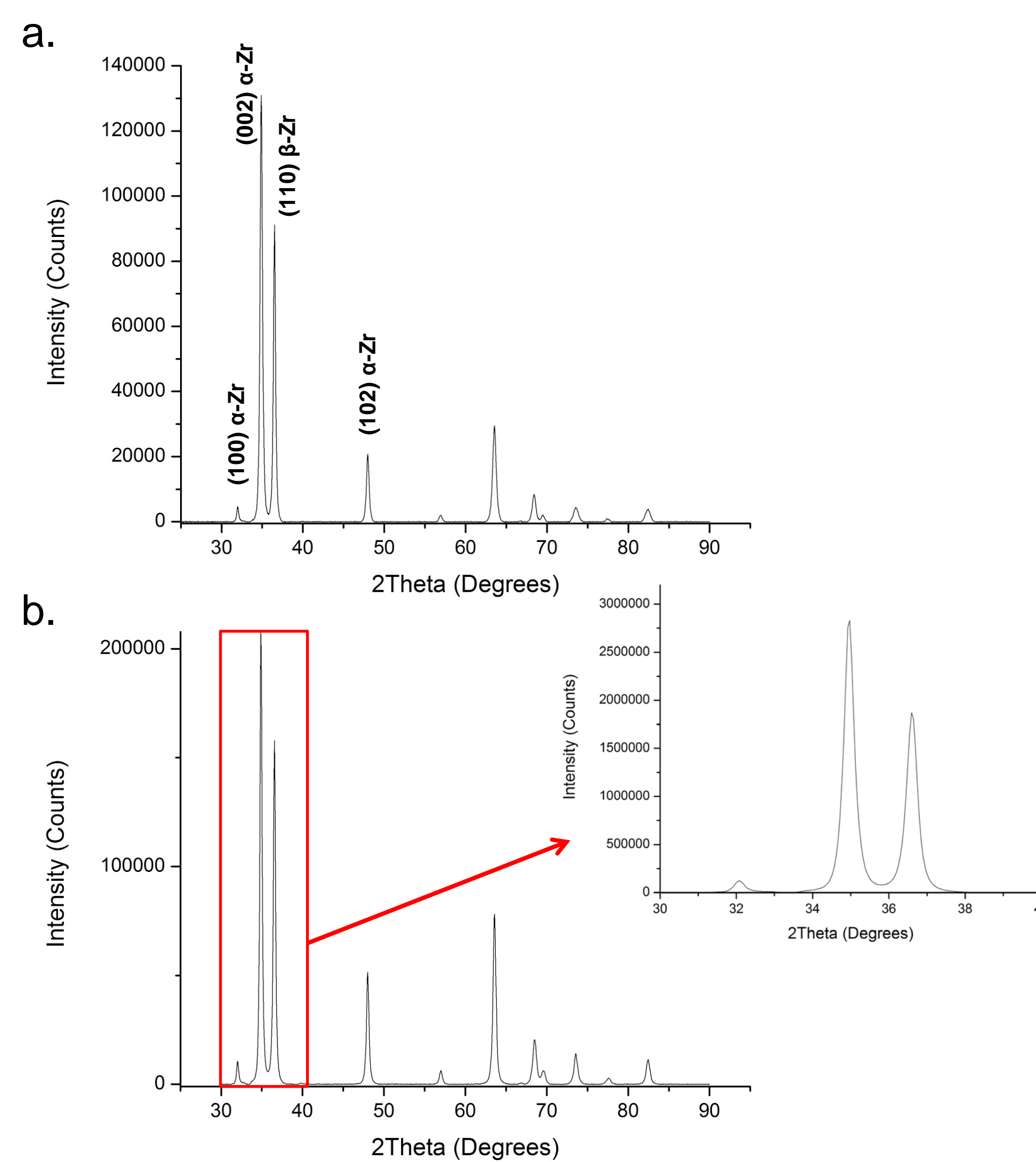


Figure 3: XRD spectra of a)  $\beta$ -quenched NSF alloy 3, b.) NSF alloy 3 aged at  $620^\circ\text{C}$  for 60 mins and range of interest.

**Discussion:** The purpose of each analysis was to determine how the phase transitions depend on the aging time and temperature.

**XRD-** XRD analysis was used to determine the temperature and time at which  $\beta_{Nb}$  and other phases precipitate. Peaks corresponding to  $\beta_{Nb}$  were expected as shown in Figure 5. Evidence of the SPP,  $\beta_{Nb}$ , was not observed.

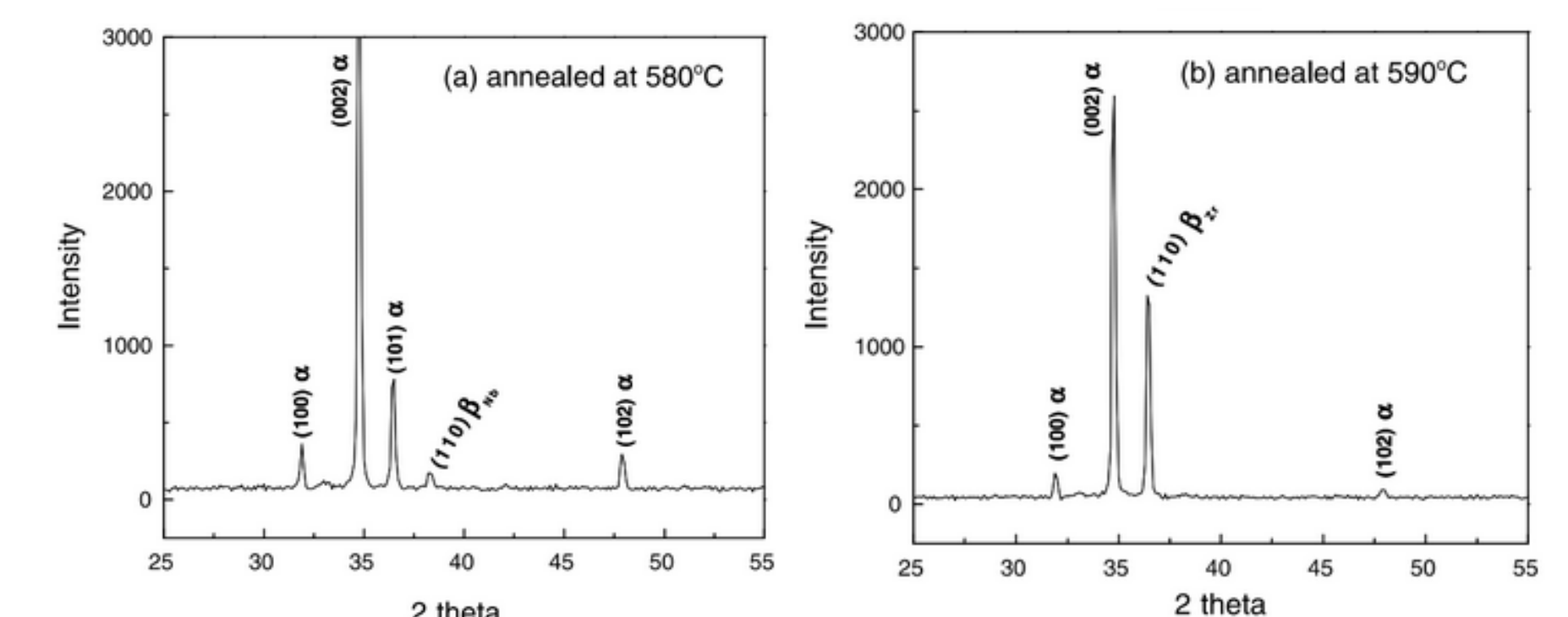


Figure 5. XRD spectra of Zr-2.0Nb alloys annealed at (a)  $580^\circ\text{C}$  and (b)  $590^\circ\text{C}$  for 3 months [5].

**DSC-** Possible evidence of the beginning of a phase transition can be seen at  $590^\circ\text{C}$  by the initiation of an exothermic peak. Further testing is currently underway using a DSC capable of a range up to  $1500^\circ\text{C}$  to gather an understanding of the full range of phase transitions.

**SEM-** Examination of the microstructure of heat-treated samples of NSF using SEM display  $\beta$  precipitates. Further investigation using TEM will allow for the determination of the composition of these precipitates. Figure 6 shows precipitates that were observed in a similar Zr alloy.

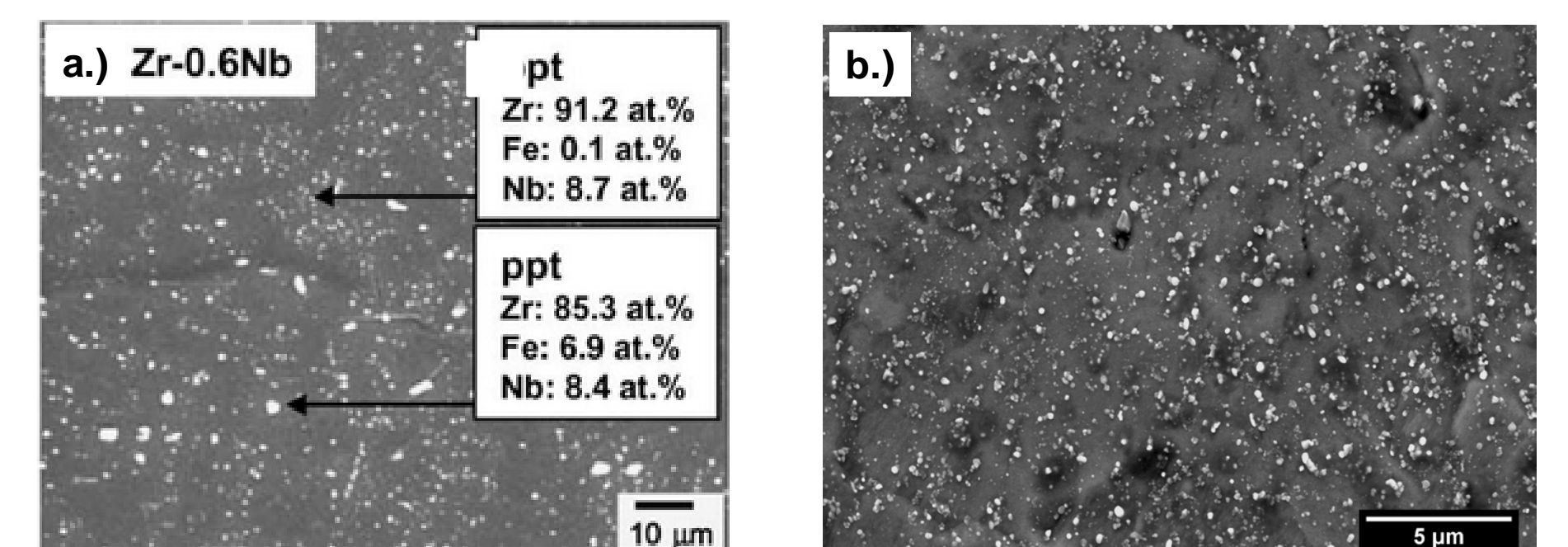


Figure 6. SEM micrograph of a.) Zr-0.6Nb alloy annealed at  $580^\circ\text{C}$  for 3 months[5], b.) SEM micrograph of NSF alloy 3 aged at  $620^\circ\text{C}$  for 20 mins.

**TEM-**

## Experimental Procedure:

Table 1: Nominal alloy compositions

Element	Alloy 1 (wt%)	Alloy 2 (wt%)	Alloy 3 (wt%)	Alloy 4 (wt%)
Zr	97.7	97.5	97.7	97.9
Nb	0.9	1.1	1.1	0.9
Sn	0.9	0.9	0.9	0.9
Fe	0.5	0.5	0.3	0.3

Table 2: Heat treatment procedures

Temperature ( $^\circ\text{C}$ )	590	620	650	670
Time (min.)	10	10	10	10
	15	15	15	15
	20	20	20	20
	60	60	60	60

Four different Zr alloys with varying chemical compositions were supplied by GNF (Table 1). Ingots of the alloys were cold rolled and then  $\beta$ -quenched. Samples were heat treated according to the procedure illustrated in Table 2. Microstructural characterization was carried out using scanning electron microscopy (SEM), transmission electron microscopy (TEM), and the phase transition behavior was investigated using differential scanning calorimetry (DSC), and x-ray diffraction (XRD).

**Differential Scanning Calorimetry:** Standard ramp analyses were performed by differential scanning calorimetry under argon gas (Auto 20 DSC, TA Instruments, Pittsburg, PA).  $\beta$ -quenched samples of each alloy composition were analyzed from  $25-700^\circ\text{C}$  at a ramp rate of  $5^\circ\text{C}/\text{min}$ . The beginning of the exothermic peak at  $\sim 590^\circ\text{C}$  corresponds to the initiation of  $\beta_{Nb}$  precipitation.

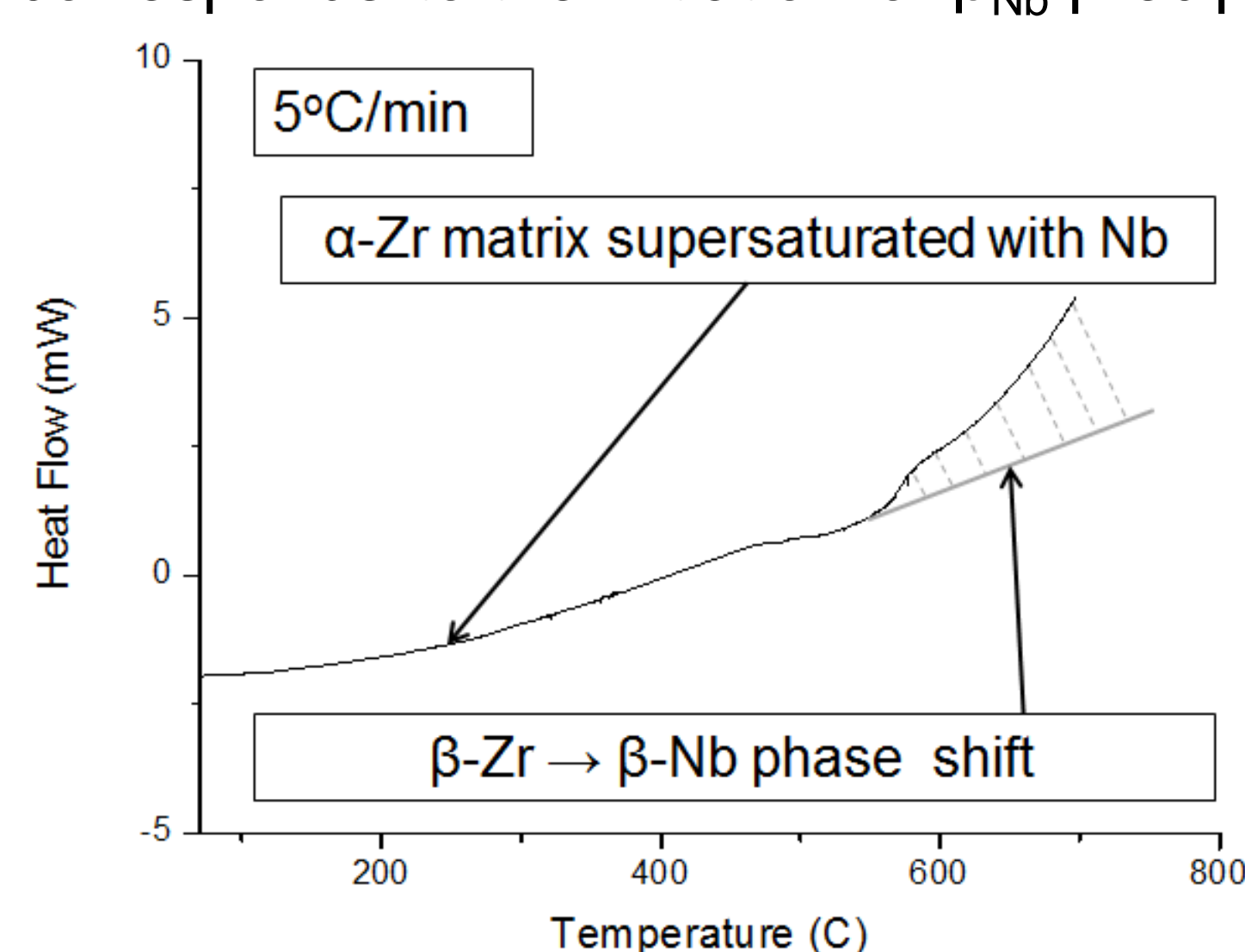


Figure 2: Thermogram obtained by calorimetry on alloy 3.

## Scanning Electron Microscopy (SEM):

Micrographs obtained are shown in Figure 4 (FEI Philips XL-40 Scanning Electron Microscope, Houston TX). The micrographs show very small Nb-containing precipitates randomly distributed in  $\alpha$  matrix. The composition of the precipitates will be analyzed by EDS in TEM.

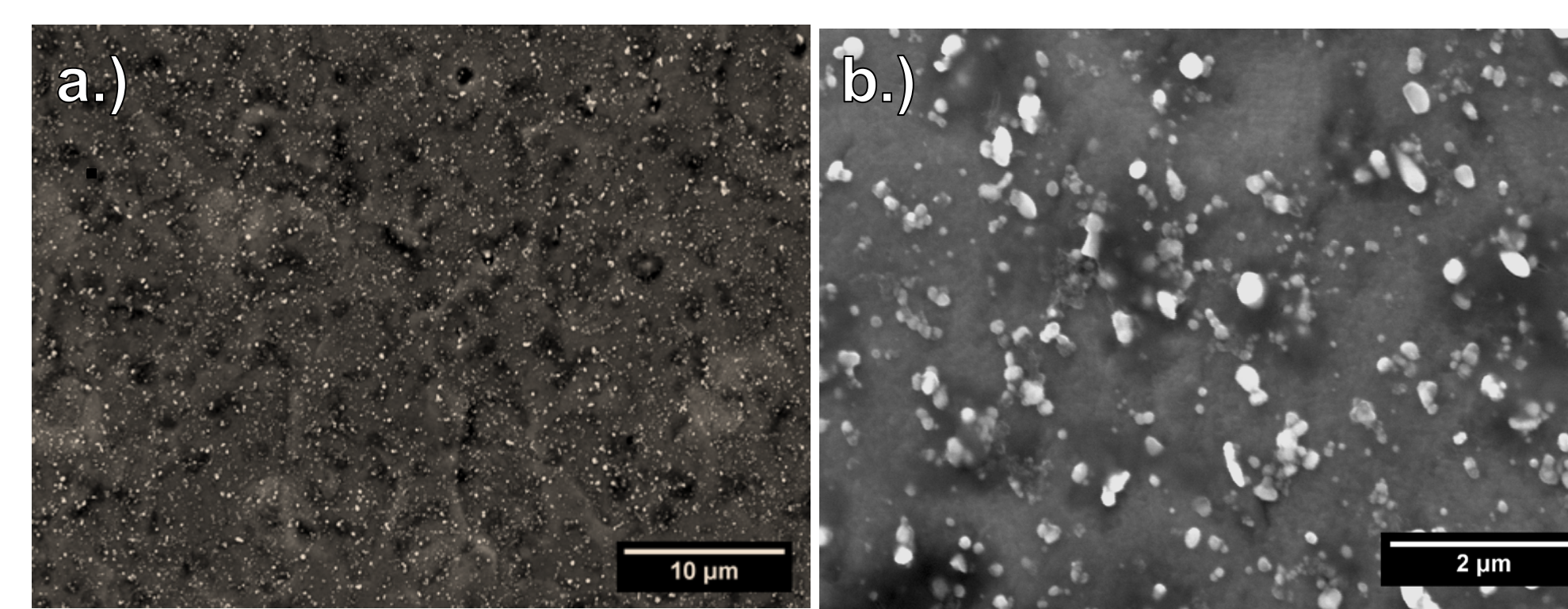


Figure 4: SEM micrographs of NSF alloy 3 aged at  $620^\circ\text{C}$  for 20 mins a.) at 2500x magnification and b.) at 15,000x mag.

## Transmission Electron Microscopy (TEM):

TEM sample preparation was performed using a FEI Nova 200 NanoLab DualBeam<sup>TM</sup>-SEM/FIB. TEM images were collected with a Titan 80-300 kV Environmental Transmission Electron Microscope (Houston TX).

**Recommendations:** Etchant to be used on these samples must be optimized to obtain more detailed information from the microstructure using optical microscopy and scanning electron microscopy. DSC should be performed up to  $1500^\circ\text{C}$  in order to see entire range of phase transition. Further TEM analysis will confirm the presence and composition of  $\beta_{Nb}$  and/or other precipitates.

## References

- [1] Granovsky, M. S., Canay, M., Lena, E., & Arias, D. (2002). Experimental investigation of the Zr corner of the ternary Zr-Nb-Fe phase diagram. *Journal of Nuclear Materials*, 302(1), 1–8.
- [2] Eagleson, Mary. *Concise Encyclopedias Chemistry*. Berlin: Walter De Gruyter, 1994. Print.
- [3] P.E. Cantonwine, Y.P. Lin, D. R. Lutz, D. W. White, K. L. Ledford, et al. BWR Corrosion Experience of NSF. TopFuel 2013, Charlotte, North Carolina, 2013.
- [4] Jeong, Y. H., Kim, H. G., & Kim, T. H. (2003). Effect of  $\beta$  phase, precipitate and Nb concentration in matrix on corrosion and oxide characteristics of Zr-xNb alloys. *Journal of Nuclear Materials*, 317(1), 1–12.
- [5] Hyun-Gil Kim, Jeong-Yong Park, Yong-Hwan Jeong. *Phase boundary of the Zr-rich region in commercial grade Zr-Nb alloys*. *Journal of Nuclear Materials*. Vol.347. 2005.

**Acknowledgements:** We would like to give a special thanks to Yang-Pi Lin, Prof. Coughlan, Jameson Root, Sung Hwan Hwang, Rosa Diaz, and Garrett Hunt for their time and help with this project.